Available online at www.sciencedirect.com

ScienceDirect

Procedia Computer Science 159 (2019) 524–533

Procedia Computer Science

www.elsevier.com/locate/procedia

23rd International Conference on Knowledge-Based and Intelligent Information & Engineering Systems

Overlapping Chromosome Segmentation using U-Net: Convolutional Networks with Test Time Augmentation

Hariyanti Mohd Saleh[a,b], Nor Hidayah Saad[a,b], Nor Ashidi Mat Isa[a]*

[a]*Imaging and Intelligent System Research Team, School of Electrical and Electronic Engineering Campus, Universiti Sains Malaysia, Nibong Tebal 14300, Malaysia*

[b]*School of Microelectronic Engineering, Universiti Malaysia Perlis, Pauh Putra Campus, 02600 Arau, Perlis, Malaysia.*

Abstract

An effective human metaphase chromosome analysis system can be used by doctors as a second opinion during diagnosis. Segmentation is necessary in developing this system to identify and distinguish between individual chromosomes. The main challenge in chromosome segmentation is the separation of overlapping chromosomes. Deep convolutional neural networks have been widely used for medical segmentation, especially with U-Net. This study investigated how Test time augmentation with a suitable number of U-Net layers can improve the design for this semantic segmentation problem. The proposed architecture was trained, validated and tested with 13,434 greyscale images with 88 × 88 pixels of overlapping chromosome pairs. With the implementation of the proposed method, the training result became more accurate without any mislabelling and additional pre-processing became unnecessary. An improved segmentation accuracy of 99.68% was obtained, which was higher than the 99.22% obtained using the method of Hu et al.

Keywords: Overlapping chromosome segmentation; U-Net; Convolutional neural networks; Test time augmentation; Deep learning

* Corresponding author. Tel.: +6045996051; fax: +6045941023.
E-mail address: hariyanti@unimap.edu.my, ashidi@usm.my

10.1016/j.procs.2019.09.207

1. Introduction

A healthy human cell image contains 46 chromosomes. The first 22 pairs of chromosomes are called autosomes and the 23rd pair are sex chromosomes called X and Y [1]. The presence of two X chromosomes represents a female, whilst XY represents a male. During metaphase, chromosomes align on the metaphase plate in the middle of the cell where the chromosome centromere, telomere and nucleolar organiser regions are located. On the basis of the centromere position of each chromosome pair which represents the relative length of the chromosome, 44 autosomes are numbered from 1 to 22 in descending order of length of each karyotype test (one exception is chromosome 21, which is shorter than chromosome 22). Fig. 1(a) shows a metaphase Giemsa-stained microscopic image, and Fig. 1(b) shows the karyotyping result of paired and ordered chromosomes. Karyotyping is the main method used to identify and evaluate the size, shape and number of chromosomes in a body cell. Major genetic disorders and chromosomal abnormalities can be diagnosed from karyotyped images. Cells divide and reproduce in two ways: mitosis and meiosis. A chromosomal abnormality sparks from a chromosomal mutation which can occur before, during and after mitosis and meiosis [2]. Klinefelter syndrome is a trisomy disorder characterised by an extra X chromosome in males. Klinefelter can stop sperm production. Other examples of trisomy are Patau syndrome (trisomy 13), Edward's syndrome (trisomy 18) and Down syndrome (trisomy 21). Down syndrome causes mental retardation. Conventional karyotyping is a difficult and time-consuming task manually performed by cytologists [3], wherein chromosomes are classified from cut paper pictures. The tediousness of this process led to the development of automatic karyotyping, also known as the chromosome classification system. Automatic karyotyping is a process of ordering and classifying chromosomes into their respective classes using computers [3]. However, cytologists need to manually drag each chromosome image to the target position. This process can still can be improved in terms of time and costs through machine learning systems. Automatic karyotyping includes four processing stages, namely image enhancement, chromosome segmentation and alignment, feature extraction and chromosome classification [4]. One of the most crucial stages during karyotyping is segmentation, which involves grouping the important features of chromosomes. The main objective of segmentation is to extract chromosomes from the background and disentangle them. However, some chromosomes overlap, which makes the separation process difficult. Overlapping chromosomes should be separated to ensure that the physical characteristics of any individual chromosome can be segmented correctly. This procedure ensures zero loss of information during feature extraction and accurate extraction of physical chromosome characteristics, such as chromosome size, centromeric index, shape profile and banding patterns.

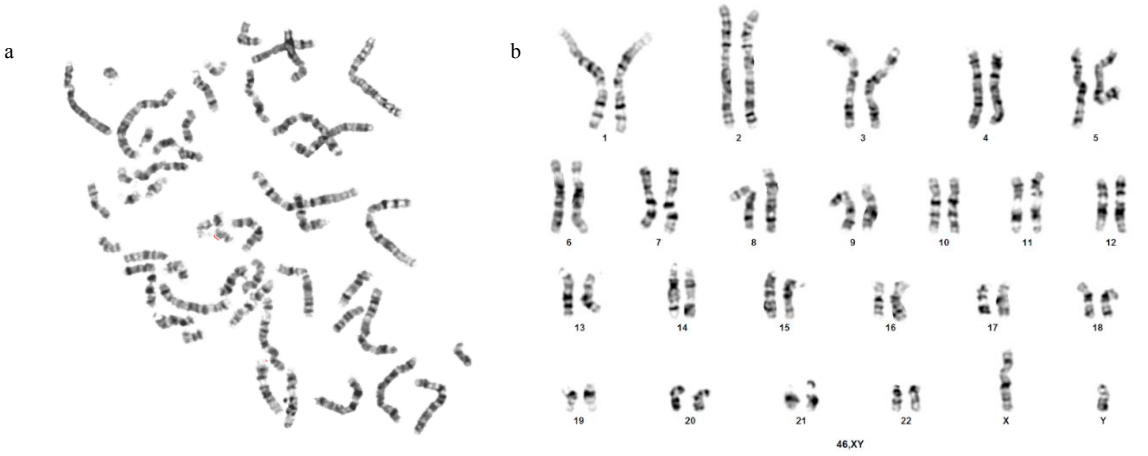

Fig. 1. (a): A metaphase Giemsa-stained microscopic image; Fig. 1. (b): Karyotyping result of paired and ordered chromosomes.

Artificial neural network (ANN) is a mathematical biology model consisting of a group of artificial neurons. Multiple layers of these neurons are called the multilayer perceptron [5]. ANN can learn from data through a training process. It is often categorised as a supervised machine learning algorithm because the training is usually done based on the labels assigned to the data. ANNs are applied to solve various classification, prediction and control problems because of its powerful learning ability. However, as the pattern complexity increases, the pattern recognition ability of ANN worsens, especially when numerous patterns need to be trained [6]. A large structure demands extensive computation and pushes the model to memorise the training instead of generalising from it. This condition leads to overfitting during the learning [6], thereby decreasing the training accuracy.

On the contrary, ANN can recognise patterns excellently when used for deep learning (DL) because DL can break complex patterns into simpler ones [7]. In the past, insufficient resources hindered the fast completion of training, but nowadays, as technology advances, central and graphics processing units have become more efficient and high-performing at affordable costs. Therefore, DL can be trained more quickly and effectively within just a few hours. DL carries a convolutional neural network (CNN), which is a class of deep neural networks commonly used for image processing. CNN is simple and easy to use. When dealing with multi-dimensional computer vision problems or meeting complex patterns such as a thousand human faces, CNN can break down the processing task [8]. For example, CNN can detect simple features such as edges and combine them to form facial features, like a nose and eyes to construct a face. With this capability, CNN is the best choice for achieving improved generalisation performance and accuracy compared to its peer. The three main types of CNNs layers are convolutional, pooling and fully connected (FC) layers. CNN drops FC layers from the main body of the architectures and introduces a mixture of convolutional and pooling layers [9]. These two layers are stacked, and the convolutional layers carry out convolutions to extract the features from the inputs to produce the feature maps.

1.1. Related Work

Numerous segmentation methods have been developed for metaphase chromosome analysis. Special segmentation methods must be applied in touching and overlapping chromosome separation owing to its complexity. Several existing methods are based on the detection of the medial axis, detecting the centerline and partitioning the centromere. These methods are performed by calculating the chromosome thickness [10]. However, if chromosome bending exists, the width tightening on higher banded chromosomes can be easily overlooked. Inaccurate calculations near the telomeric region of chromosomes can be committed while chromosomes are separated from their sister chromatids. Ji [11] proposed a rule based on contour analysis to force the image to contain a reasonable number of chromosomes. However, the method was only able to segment a limited profile in an image. Somasundaram and Kumar [12] separated overlapping chromosomes by estimating a cut point on an image to cut the overlapping region, but this separation caused loss of details. Watershed transform [13–14] can also be applied but only after the segmentation of the noise is increased. Madian et al. [15] identified the concave points on the image contour and developed heuristics for chromosome separation. Cao et al. [16] developed an adaptive fuzzy c-means to segment the chromosomes. This method had the advantage of correcting the non-uniform illumination caused by the microscope imaging system and a good segmentation algorithm that can segment the touching and overlapping chromosomes in different illumination regions. However, this method is limited only to the analysis of multicolour fluorescence in situ hybridisation (M-FISH) images. Given the combinatorial nature of reassembling pieces, Grisan et al. [17] segmented chromosomes using a space-variant thresholding scheme and developed a tree search of choices to resolve touching and overlapping chromosomes. However, the high variability in chromosome fluorescence intensity rendered the threshold impractical [17]. When histograms were plotted for two overlapping chromosomes, a substantial overlap appeared between the histograms. Thus, threshold pixel is not an appropriate measure for segmenting overlapping chromosomes [18].

DL has been widely used in image segmentation. As chromosomes are part of human cells, cell segmentation is the closest topic to image segmentation and its related works will be discussed in this section. Accurate cell information is very important because one small discrepancy will affect disease analysis. Thus, researchers have utilised deep CNN for cell segmentation [19]. Song et al. modelled cell segmentation with a multi-scale CNN [20].

Yang et al. successfully used Fully convolutional neural network (FCNN) with an iterative k-terminal cut algorithm for glial cell segmentation [21]. Akram et al. demonstrated a cell bounding box proposal and used FCNN for cell segmentation [23]. Spatial information is essential for achieving good cell segmentation accuracies. Thus, Hatipoglu et al. [22] used the spatial and contextual relationships of extracellular and cellular pixels to conduct cell segmentation by creating various pixels in a window structure to contain the neighbours of a pixel [22]. Cell segmentation in breast tissue has also been studied using DL algorithms [24, 25]. Olaf successfully modelled a cell segmentation using U-Net with deformation augmentation [26]. To create a U-shaped network architecture, the U-Net architecture extended the fully convolutional network (FCN) by adding a symmetric upsampling to a down-sampling path.

Several researchers have conducted touching and overlapping chromosome segmentation with CNN. Esteban et al. [27] used FCN for semantic segmentation to segment the M-FISH of chromosome images. The architecture scored a coordinated cluster representation of 87.41%. Pommier et al. [28] [29] successfully generated the 13,434-groundtruth and greyscale of overlapping chromosome pairs. They performed prediction segmentation and compared it with the groundtruth. Pommier's dataset was then utilised by two other researchers [18] [30]. Ghosh et al. [30] applied U-Net by mixing both categories of pixels belonging to non-overlapping chromosomes. Originally, they divided the labels into four classes: a background, two non-overlapping pixels and an overlapping pixel. Their analysis obtained a prediction result of 81%. Then, they combined two non-overlapping pixels to decrease the classes to three. With the labels combined, the result of predicted mask accuracy was 97%. Hu et al. [18] reduced U-Net layers to match the input. Inputs in greyscale pairs were converted to three channel checkpoints and groundtruth labels were generated by adding masks and labelling them as chromosome 1, chromosome 2 and overlapping. The prediction results achieved an intersection over union (IOU) score of 94.7% for the overlapping region and 88%–94% for the non-overlapping regions. The current work utilises the U-Net architecture because of its success in cell imaging and chromosome segmentation.

2. Proposed Method

2.1. Dataset and Groundtruth Segmentation Process

A dataset of overlapping chromosome is built to obtain a large number of datasets. A set of human metaphases is collected using a Cy3 fluorescent telomeric probe. Blue 4′,6-Diamidino-2-phenylindole, which is a chromosome, and Orange Cy3, which focuses on telomere images of the chromosome image, are combined into a greyscale image. The resolution is decreased by two because images with a smaller resolution are easier to analyse. Chromosome overlapping is done by selecting a pair of two greyscale chromosome images. One of the greyscale chromosome images is rotated either vertically or horizontally to accommodate its pair. Masks are added to each chromosome to generate a groundtruth. The greyscale pairs are labelled to three channel checkpoints, value 1 for the first chromosome, value 2 for the mask of the other chromosomes and value 3 for the overlapping region. A total of 13,434 greyscale images with 94 × 93 pixels are generated to demonstrate overlapping chromosome segmentation. Raw images of dataset are available in Kaggle and Github [28] [29]. However, the present study applies Pommier's new clean dataset which produced different results from the analysis of the previous method.

We assign an object class for each pixel in the image for semantic segmentation. However, before semantic segmentation, greyscale image pairs are reshaped and standardised to 88 × 88 pixels to match the pooling layers with strides of two and make the dimensions divisible by two. Fig. 2 shows the groundtruth segmentation process from the full-resolution image. In the segmentation map, blue represents the background, which is labelled as 0. Label 1 in yellow represents the non-overlapping region of the first chromosome, whilst Label 2 represents the non-overlapping region of the second chromosome. Red areas labelled as 3 represent the overlapping region.

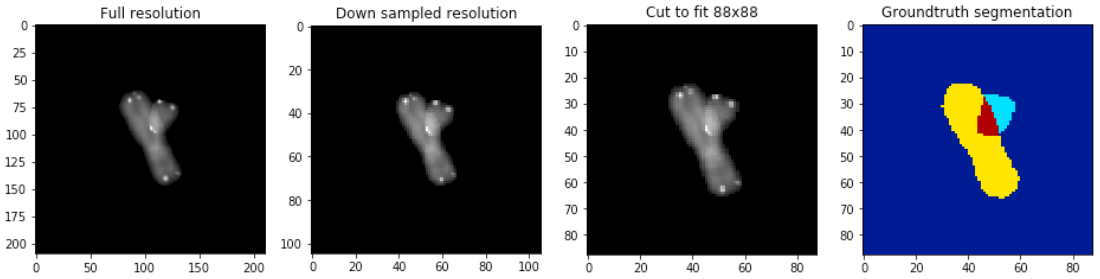

Fig. 2: Sample of groundtruth segmentation process

2.2 Proposed Network Structure

The implemented model is the modified version of the U-Net architecture constructed by Olaf et al. [26]. The proposed architecture is used to train the image dataset. The architecture of U-Net consists of two paths. The first path builds an abstract representation of the image by iteratively convolving and subsampling the images, and the second one creates the target segmentation map by iterative upsampling and convolving the abstract feature maps [26]. These paths are symmetrical and connected by concatenating the corresponding upsampling and downsampling layers. The U-Net network is known as highly invariant (never changes), and it provides a stable and precise segmentation result because of its shape, wherein the features of images are merged to give high-resolution results. Moreover, pooling operators are replaced by upsampling operators to increase the resolution of the output. Adding more layers will help extract additional features for input data and eventually increase accuracy. However, there are limits at some point; specifically, instead of extracting features, overfitting can occur and lead to system error [31] [32]. The result may show signs of overfitting while U-Net conducts the training. One way of fixing this problem is by using test time augmentation (TTA).

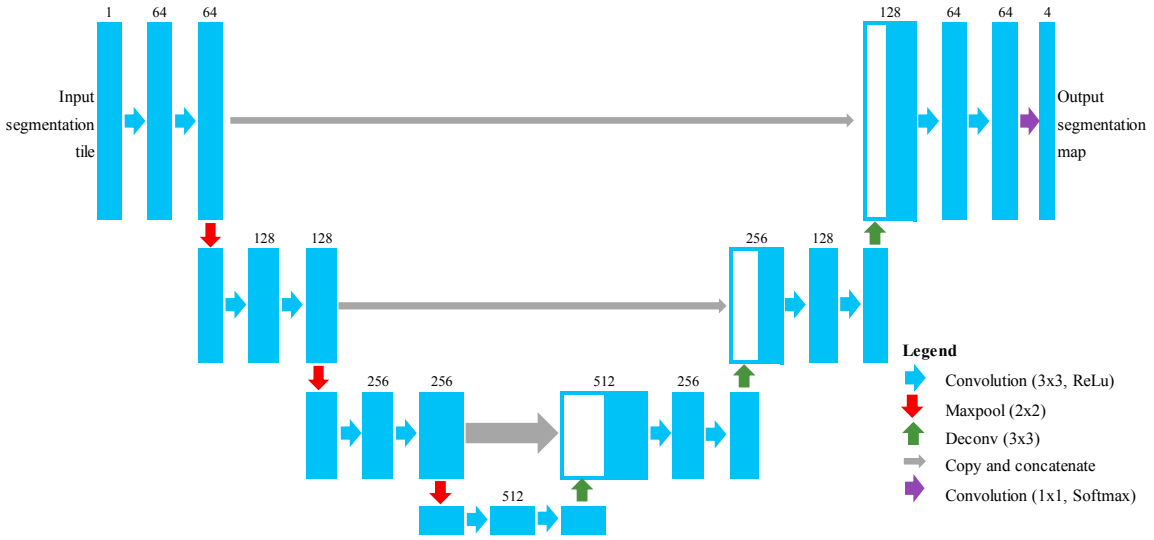

Fig. 3: Proposed U-Net architecture for chromosome segmentation. Each blue box corresponds to a multi-channel feature map, while the white boxes are the copied feature maps.

For the proposed method, the repeated convolutional network is used in the contracting path. This network is characterised by a repeated application of two 3 × 3 unpadded convolutions. Each convolution is followed by a rectified unit and a 2 × 2 max pooling operation and is supported with stride 2. The purpose of the contracting path is to capture the input image. The information feature increases by going through each layer. Four concatenations

are performed in this architecture. Except for the concatenation axis, a concatenate layer requires inputs with matching shapes. For example, layers with 22 × 22 pixels (none, 22, 22, 512) can only concatenate with another. The batch size is 2, padding is set to be the 'same' and there is one optional softmax layer at the end. Cropping can be done, but for this case, it is not given the small input image; thus, removing the pixels is undesirable. The proposed method is an improvised version of Hu et al.'s [18] method with additional CNN layers and TTA. As shown in Table 1, the proposed architecture has more multi-channel feature map numbers and layers compared to Hu et al.'s architecture [18]. However, the proposed architecture has less multi-channel feature map numbers and layers to match the input compared to the original U-net architecture [26]. The proposed architecture has a maximum of 512 channels before deconvolution compared to the 256 channels in Hu et al.'s [18] architecture, whilst the original U-Net architecture has 1024 channels [26].

TTA was implemented in the proposed model on the basis of work done by [33]. However, we only applied horizontal and vertical image flipping to limit the training time duration. In general, implementing TTA increases the chances of capturing a variety of objects because the model has been fed with overlapping chromosomes in different shapes. Thus, the model can learn more cases with different sizes, angles and locations. With the help of TTA, models become more intelligent in capturing and generalising overlapping chromosomes because of their exposure to more aspects of the data.

TTA modifies and multiplies the training data during the training. The number of different images will increase but the number of additions is unknown because image augmentation happens while training. Owing to this phenomenon, the total number of images per epoch stays the same. Augmentation is randomly applied after every epoch. Hence, an epoch does not look the same as the epoch before because the model has never seen the image as the same image twice. A total of 15 epochs are used for training and Keras Python library using TensorFlow backend is used for DL.

Table 1. Summary of the network structure of overlapping chromosome by Olaf et al. [26], Hu et al. [18], Hu et al. with TTA and the proposed method.

Method	Architecture
Olaf et al. [26]	Multi-channel feature map is up to 1024 channels before deconvolution process.
Hu et al. [18]	Multi-channel feature map is up to 256 channels before deconvolution process.
Hu et al. + TTA	Multi-channel feature map is up to 256 channels before deconvolution process.
Proposed method	Multi-channel feature map is up to 512 channels before deconvolution process. Architecture has less multi-channel feature map numbers and layers compared to the original U-net architecture [26] but more multi-channel feature map numbers and layers compared to Hu et al.'s architecture [18]. TTA also being implemented.

3. Results

This section presents the experimental results in three parts: (1) training result of overlapping chromosome training which runs with 15 epochs each, (2) segmentation result of overlapping chromosome prediction and groundtruth comparison and (3) the score of segmentation results. Hu et al.'s methods (with and without TTA) and the proposed method are implemented. The comparison of the proposed method with the previous method is discussed along the way.

Fig. 4 shows the examples of overlapping chromosome training results by Hu et al. [18] without (a) and with TTA (b) and the proposed method (c). The first column is the background image, followed by the first chromosome at the second column, the second chromosome at the third and the overlap region at the fourth. The rows represent the four pairs of overlapping chromosomes. The image on the first row focuses mainly on a single pair of chromosomes. The first pair on the first row and the second pair on the second row have no significance differences. However, the pair on the third and fourth rows shows a mislabelled area for the second chromosome which can be seen in the third column [Figs. 4(a) and 4(b)]. Fig. 4(c) illustrates how the proposed method solves the issue. The

training result is accurate and contains no mislabelling. Therefore, additional pre-processing is not necessary after implementing the proposed method.

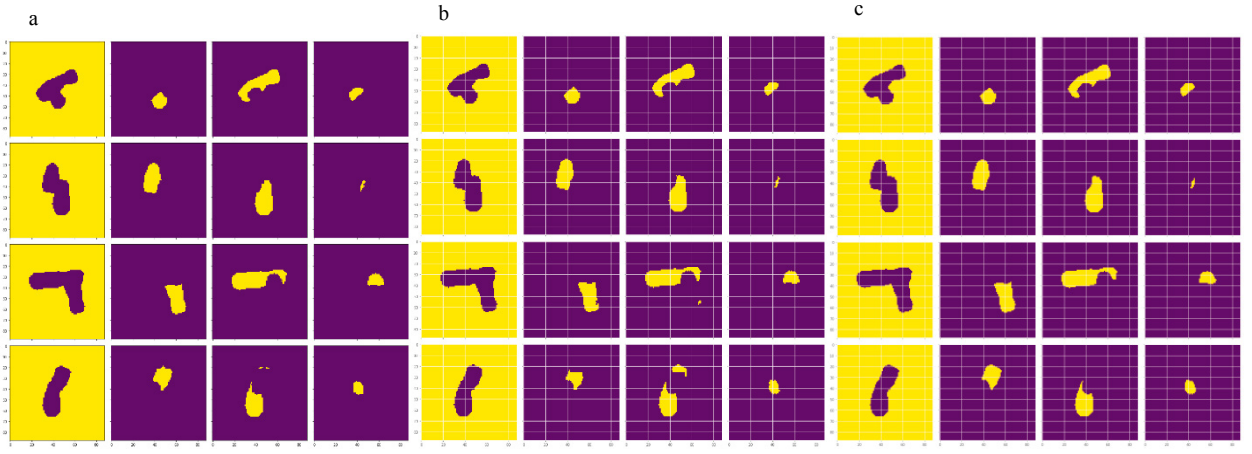

Fig. 4. (a): An example of overlapping chromosome training result obtained by Hu et al. [18]; (b): An example of overlapping chromosome training result obtained by Hu et al. with TTA; (c): An example of overlapping chromosome training result obtained by the proposed method

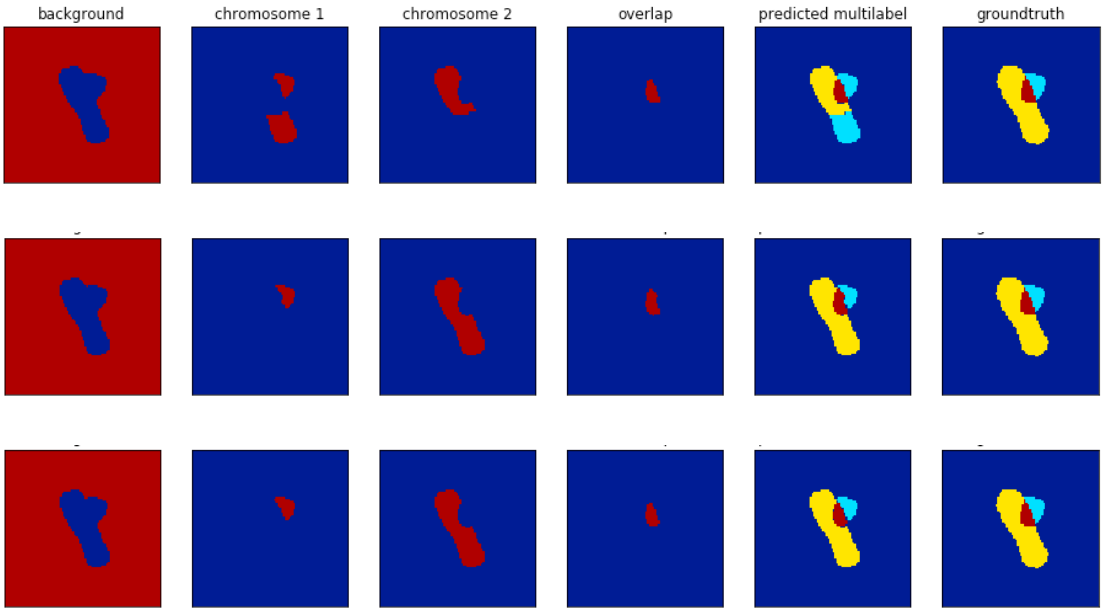

Fig. 5: The first row shows the segmentation results of overlapping chromosome prediction and groundtruth comparison by Hu et al. [18]. The second row shows the segmentation result of overlapping chromosome prediction and groundtruth comparison obtained by Hu et al. with TTA. The third row shows the segmentation results of overlapping chromosome prediction and groundtruth comparison obtained by the proposed method.

Fig. 5 shows the segmentation results of Hu et al. [18] (with and without TTA) and the proposed method from a visualised perspective. The images consist of the backgrounds and images of the first and second chromosomes and the overlap region. The predicted multilabel can be obtained by combining all four images and regions. The initial output of Hu *et al.* [18] is found to be noisy and inaccurate for the predicted multilabel because of the huge region of

mislabelling in the segmentation of the first and second chromosomes. A big part of the second chromosome is mistakenly segmented as the first chromosome. At the third row, after the implementation of TTA and additional layers, the result of predicted multilabel significantly improves and becomes more spatially consistent when compared to the groundtruth, whereas when the proposed method is applied, an even smoother and more accurate segmentation is obtained.

Table 2 shows the segmentation results of Hu et al. [18] (with and without TTA) and the proposed method on the percentage of training and testing IOU for overlapping pixels. IOU is calculated to access the result quantitatively and is defined as the area of overlap divided by the area of union (between the prediction and the groundtruth) [11] (Fig. 6). The achievable range of IOU for overlapping pixels (90.63%–99.94%) is significantly better in the proposed method than in the methods of Hu et al. (78.93%–99.93%).

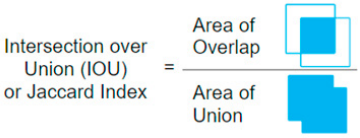

Fig.6: Definition of intersection of union

Table 2: IOU ranges for training and testing obtained by the three methods

Method	Training IOU Range (%)	Testing IOU Range (%)
Hu et al. [18]	88.87–99.94	78.93–99.93
Hu et al. + TTA	90.86–99.94	80.10–99.94
Proposed method	91.49–99.95	90.63–99.94

Table 3 presents the quantitative evaluations for the three methods. The initial outputs of overlapping chromosome training and testing segmentation are 99.57% and 99.22%, respectively. After using TTA, the scores become 99.63% and 99.27%, respectively. When the proposed method is used, higher accuracies are obtained, 99.79% for training and 99.68% for testing.

In conclusion, the proposed architecture design with additional layers and feature extraction channel extracts more features for input data and eventually enhances the accuracy compared with the previous designs. When TTA is applied for the training dataset, the transformation of images gives the model higher chances of capturing the target shape of overlapping chromosomes, thereby improving the prediction process or test images and the testing accuracy. This is how it works in improving the semantic segmentation accuracy of Hu et al.'s result.

Table 3: Segmentation results of overlapping chromosome training and testing accuracy

Method	Training accuracy (%)	Testing accuracy (%)
Hu et al. [18]	99.57	99.22
Hu et al.+ TTA	99.63	99.27
Proposed method	99.79	99.68

4. Conclusion and Future Work

In this work, U-Net architecture was modified by adding a suitable number of layers and implementing TTA to perform the overlapping chromosome semantic segmentation task. The proposed method can fix mislabelling issues while carrying out the training. As a result, additional pre-processing is not necessary and the accuracy of segmentation increases compared to that of Hu et al.'s previous work The proposed architecture improves the

performance of chromosome segmentation in all areas: visualisation, quantitative training and testing (IOU and accuracy). For future work, we aim to further improve the accuracy. An opportunity to use instance segmentation and dedicated algorithm for the model may also arise.

Acknowledgements

This work was supported by the Universiti Sains Malaysia Research University (Individual) Research Grant Scheme under Grant 1001/PELECT/8014030 entitled “Development of Automatic Intelligent Karyotyping System of Classifying Abnormal Chromosome”.

References

[1] Jean McGowan-Jordan, Annet Simons, Michael Schmid, ISCN .2016. An International System for Human Cytogenomic Nomenclature, Karger
[2] Susan Mahler Zneimer, 2014. Cytogenetic Abnormalities (Chromosomal, FISH and Microarray-Based Clinical Reporting), Wiley Blackwell.
[3] Harold Chen, 2006. Atlas of Genetic Diagnosis and Counseling Humana Press.
[4] Marilyn S.Arsham, Margaret J.BArch, Helen J.LAwce . 2017. The AGT Cytogenetics Laboratory Manual (4th Edition), Wiley Blackwell
[5] Sodhi, S. S. and Chandra, P.2014. Bi-modal Derivative Activation Function for Sigmoidal Feedforward Networks. Neurocomputing. 143: 182–196.
[6] Almási, A.-D., Woz´niak, S., Cristea, V., Leblebici, Y. and Engbersen, 2016. T. Review of Advances in Neural Networks: Neural Design Technology Stack. Neurocomputing. 174, Part A: 31–41.
[7] LeCun, Yann; Bengio, Yoshua; Hinton, Geoffrey .2015. "Deep learning". Nature. 521 (7553): 436–444
[8] Chopra, S., Hadsell, R. and LeCun. 2005.Y. Learning A Similarity Metric Discriminatively with Application to Face Verification. Computer Vision and Pattern Recognition. CVPR 2005. IEEE Computer Society Conference on., vol. 1
[9] Krizhevsky, A., Sutskever, I., Hinton, G.E. 2012. Imagenet classification with deep convolutional neural networks. Advances in neural information processing systems, pp. 1097–1105, 2012
[10] A. S. Arachchige, J. Samarabandu, J. H. Knoll, and P. K. Rogan. 2013. Intensity integrated laplacian-based thickness measurement for detecting human metaphase chromosome centromere location. IEEE Transactions on Biomedical Engineering, vol. 60, no. 7, pp. 2005–2013.
[11] Ji, L., 1994. Fully automatic chromosome segmentation. Cytometry Part A, 17(3), pp.196-208.
[12] Somasundaram, D. and Kumar, V.V. 2014. Separation of overlapped chromosomes and pairing of similar chromosomes for karyotyping analysis. Measurement, 48, pp.274-281.
[13] Karvelis, P.S., Fotiadis, D.I., Syrrou, M. and Georgiou, I.,2005. Segmentation of chromosome images based on a recursive watershed transform. In IFMBE Proc vol. 11, No. 1, pp. 1727-1983.
[14] Karvelis, P., Likas, A. and Fotiadis, D.I., 2010. Identifying touching and overlapping chromosomes using the watershed transform and gradient paths. Pattern Recognition Letters, 31(16), pp.2474-2488.
[15] N. Madian and K. Jayanthi. 2014. Analysis of human chromosome classification using centromere position,” Measurement, vol. 47, pp. 287–295, 2014.
[16] Cao, H., Deng, H.W. and Wang, Y.P. 2012. Segmentation of M-FISH images for improved classification of chromosomes with an adaptive fuzzy C-means clustering algorithm. IEEE transactions on fuzzy systems, 20(1), pp.1-8.
[17] Grisan, E., Poletti, E. and Ruggeri, A., 2009. Automatic segmentation and disentangling of chromosomes in Q-band prometaphase images. IEEE Transactions on Information Technology in Biomedicine, 13(4), pp.575-581.
[18] Hu, RL, Karnowski, J, Fadely, R, Pommier, JP.Neural. 2017. Image Segmentation to Distinguish Between Overlapping Human Chromosomes”, Information Processing Systems Machine Learning for Health Workshop.
[19] Litjens, G. J. S., Kooi, T., Bejnordi, B. E., Setio, A. A. A., Ciompi, F., Ghafoorian, M., van der Laak, J. A. W. M., van Ginneken, B. & Sánchez, C. I. 2017. A survey on deep learning in medical image analysis. Medical Image Analysis, 42, 60-88.
[20] Song, Y., Zhang, L., Chen, S., Ni, D., Lei, B., Wang, T. 2015. Accurate segmentation of cervical cytoplasm and nuclei based on multiscale convolutional network and graph partitioning. IEEE Trans Biomed Eng 62 (10), 2421–2433.
[21] Yang, L., Zhang, Y., Guldner, I.H., Zhang, S., Chen, D.Z. 2016 .3d segmentation of glial cells using fully convolutional networks and k-terminal cut. In: Med Image Comput Comput Assist Interv. Vol. 9901 of Lect Notes Comput Sci. Springer, pp. 658–666.
[22] Akram, S. U., Kannala, J., Eklund, L., Heikkil¨a, J. 2016. Cell segmentation proposal network for microscopy image analysis. In: DLMIA. Vol. 10008 of Lect Notes Comput Sci. pp. 21–29.
[23] Hatipoglu, Nuh & Bilgin, Gökhan. 2017. Cell segmentation in histopathological images with deep learning algorithms by utilizing spatial relationships. Medical & Biological Engineering & Computing. 55.
[24] Petersen K, Nielsen M, Diao P, Karssemeijer N, Lillholm M. 2014. Breast tissue segmentation and mammographic risk scoring using deep learning. In: Breast imaging: proceedings of 12th international workshop on digital mammography, IWDM’14. Springer, Berlin, pp 88–94
[25] Xu J, Luo X, Wang G, Gilmore H, Madabhushi A. 2016. A deep convolutional neural network for segmenting and classifying epithelial and stromal regions in histopathological images. Neurocomputing 191:214–223
[26] Olaf Ronneberger, Philipp Fischer, and Thomas Brox .2015. U-net: Convolutional networks for biomedical image segmentation. In International Conference on Medical Image Computing and Computer-Assisted Intervention, pages 234–241. Springer.
[27] Esteban Pardoa, José Mário T Morgadob, Norberto Malpicaa. 2018. Semantic segmentation of mFISH images using convolutional networks, Cytometry.
[28] Pommier JP. 2016. Overlapping chromosomes. https://www.kaggle.com/jeanpat/ overlapping-chromosomes/data.

[29] PommierJP. Overlappingchromosomes. 2016. https://github.com/jeanpat/DeepFISH/tree/ master/dataset
[30] https://www.linkedin.com/pulse/segmenting-overlapping-chromosomes-using-deep-learning-rohit-ghosh
[31] Ali Sharif Razavian Hossein Azizpour Josephine Sullivan Stefan Carlsson. CNNFeaturesoff-the-shelf:an Astounding Baseline for Recognition
[32] Tara N. Sainath, Oriol Vinyals, Andrew Senior, Haşim Sak. 2015. Convolutional, Long Short-Term Memory, fully connected Deep Neural Networks. 2015 IEEE International Conference on Acoustics, Speech and Signal Processing (ICASSP)
[33] Wang G., Li W., Ourselin S., Vercauteren T. 2019. Automatic Brain Tumor Segmentation Using Convolutional Neural Networks with Test-Time Augmentation. In book: Crimi A., Bakas S., Kuijf H., Keyvan F., Reyes M., van Walsum T. (eds) Brainlesion: Glioma, Multiple Sclerosis, Stroke and Traumatic Brain Injuries. BrainLes 2018. Lecture Notes in Computer Science, vol 11384. Springer